Remote Sensing of Environment 174 (2016) 100–108

Contents lists available at ScienceDirect

Remote Sensing of Environment

journal homepage: www.elsevier.com/locate/rse

Predicting dead fine fuel moisture at regional scales using vapour pressure deficit from MODIS and gridded weather data

Rachael H. Nolan [a,b,*,1], Víctor Resco de Dios [a,2], Matthias M. Boer [a], Gabriele Caccamo [b,3], Michael L. Goulden [c], Ross A. Bradstock [b]

[a] Hawkesbury Institute for the Environment, Western Sydney University, Richmond, NSW, Australia
[b] Centre for Environmental Risk Management of Bushfires, Centre for Sustainable Ecosystem Solutions, University of Wollongong, Wollongong, NSW, Australia
[c] Department of Earth System Science, University of California, Irvine, CA 92697, USA

ARTICLE INFO

Article history:
Received 21 June 2015
Received in revised form 19 October 2015
Accepted 9 December 2015
Available online 17 December 2015

Keywords:
Remote sensing
Land surface temperature
MODIS
Wildfire

ABSTRACT

Spatially explicit predictions of fuel moisture content are crucial for quantifying fire danger indices and as inputs to fire behaviour models. Remotely sensed predictions of fuel moisture have typically focused on live fuels; but regional estimates of dead fuel moisture have been less common. Here we develop and test the spatial application of a recently developed dead fuel moisture model, which is based on the exponential decline of fine fuel moisture with increasing vapour pressure deficit (D). We first compare the performance of two existing approaches to predict D from satellite observations. We then use remotely sensed D, as well as D estimated from gridded daily weather observations, to predict dead fuel moisture. We calibrate and test the model at a woodland site in South East Australia, and then test the model at a range of sites in South East Australia and Southern California that vary in vegetation type, mean annual precipitation (129–1404 mm year^{-1}) and leaf area index (0.1–5.7). We found that D modelled from remotely sensed land surface temperature performed slightly better than a model which also included total precipitable water (MAE < 1.16 kPa and 1.62 kPa respectively). D calculated with observations from the Moderate Resolution Imaging Spectroradiometer (MODIS) on the Terra satellite was under-predicted in areas with low leaf area index. Both D from remotely sensed data and gridded weather station data were good predictors of the moisture content of dead suspended fuels at validation sites, with mean absolute errors less than 3.9% and 6.0% respectively. The occurrence of data gaps in remotely sensed time series presents an obstacle to this approach, and assimilated or extrapolated meteorological observations may offer better continuity.

1. Introduction

Fuels consumed in wildfires are comprised of dead and live plant material, with dead fine fuels of particular importance in determining the initial rate of surface fire spread and intensity (Sullivan, 2009; Viney, 1991). The water content of litter and other dead plant biomass is a strong determinant of ignition probability and the rate of spread of wildfire (Rothermel, 1983). The water content of fuel is therefore crucial for quantifying fire danger and as an input to fire behaviour models (Sullivan, 2009).

The moisture content of dead fuels (FM) is a function of fuel size, local atmospheric conditions and precipitation (Matthews, 2013; Viney, 1991). In the absence of precipitation, FM responds to changes in atmospheric conditions through water vapour sorption or desorption. FM tends to equilibrate with atmospheric humidity, with larger diameter fuel equilibrating slowly and smaller diameter fuel, such as leaf litter and woody debris with a diameter less than 25.4 mm, equilibrating rapidly (Catchpole, Catchpole, Viney, McCaw, & Marsden-Smedley, 2001; Viney & Catchpole, 1991). FM is commonly modelled from meteorological variables such as air temperature, relative humidity, rainfall, and wind speed; with solar radiation, soil moisture content and potential evapotranspiration less commonly used (Matthews, 2013). Most efforts to use remote sensing to estimate fuel moisture have focused on live fuels (e.g. Caccamo, Chisholm, Bradstock, Puotinen, & Pippen, 2012; Chuvieco et al., 2004; Stow & Niphadkar, 2007; Yebra & Chuvieco, 2009). These approaches have typically exploited relationships between surface reflectance, vegetation greenness and leaf water content (Bowyer & Danson, 2004; Ceccato, Flasse, & Gregoire, 2002). For dead fuels, FM has been indirectly predicted from remotely

* Corresponding author at: Hawkesbury Institute for the Environment, Western Sydney University, Richmond, NSW, Australia.
E-mail address: Rachael.Nolan@uts.edu.au (R.H. Nolan).
[1] Current address: Terrestrial Ecohydrology Research Group, School of Life Sciences, University of Technology Sydney, Broadway, NSW, Australia.
[2] Current address: Department of Crop and Forest Sciences—AGROTECNIO Center, Universitat de Lleida, E 25198 Lleida, Spain.
[3] Current address: NSW Department of Primary Industries, Parramatta, NSW, Australia.

http://dx.doi.org/10.1016/j.rse.2015.12.010
0034-4257/

sensed data by Nieto, Aguado, Chuvieco, and Sandholt (2010), who used estimates of temperature and relative humidity from the SEVIRI sensor on the MSG satellite to calculate FM across Spain using the U.S. National Fire Danger Rating System (Bradshaw, Deeming, Burgan, & Cohen, 1983) and the Canadian Fire Weather Index. However, modelled FM was only compared against predictions from on-ground meteorological data and not against directly measured fuel moisture.

Resco de Dios et al. (2015) recently proposed vapour pressure deficit (D) as a predictor of fine dead FM. In this semi-mechanistic model, FM_D, is based on the exponential decline in FM with increasing D (Resco de Dios et al., 2015). Resco de Dios et al. (2015) compared their FM_D model with eight other models, including those widely used in fire danger indices (e.g. the Keetch and Byram Drought Index (Keetch & Byram, 1968), the drought factor used in McArthur's Forest Fire Danger Index (McArthur, 1967) or the equilibrium moisture of Nelson (1984), to name a few). FM_D provided comparatively more accurate and less biased predictions of FM across a range of both fuel moisture values and contrasting environments (Resco de Dios et al., 2015).

In principle, regional scale predictions of FM may be derived by combining Resco de Dios et al.'s D-based approach with spatially gridded estimates of D based on meteorological assimilation or remote sensing. In practice, estimates of FM modelled from interpolated weather station data may be uncertain in regions where the terrain or vegetation is especially heterogeneous (Nieto et al., 2010). This problem may be overcome by predicting FM based on remotely sensed D, since satellite observations are available with a spatial resolution of 1 km^2 or finer. However, remotely sensed D may not be available at a daily time-step due to factors such as cloud cover, whereas meteorological data derived from either interpolation or climate models tend to be more continuous.

D is typically calculated from air temperature (T_{air}) and relative humidity (RH) which are used to calculate saturation vapour pressure (e_s) and actual vapour pressure (e_a) (Monteith & Unsworth, 1990):

$$e_s = 0.6108 * \exp\left(17.27 * \frac{T_{air}}{T_{air} + 237.3}\right) \quad (1)$$

$$e_a = \frac{RH}{100} * e_s \quad (2)$$

$$D = e_s - e_a. \quad (3)$$

Two main approaches have been used to calculate D from remotely sensed data. First, D can be calculated from T_{air} and e_a, with T_{air} calculated from land surface temperature (T_{LST}) and the Normalized Difference Vegetation Index (NDVI) (Goward, Waring, Dye, & Yang, 1994; Nemani & Running, 1989) and e_a from total precipitable water (W) in the atmosphere (Nieto et al., 2010; Smith, 1966). Alternatively, Hashimoto et al. (2008) developed a more parsimonious approach based on an empirical relationship between D, e_s and T_{LST}. The ability of T_{LST} to predict D is due to a feedback between T_{LST} and near-surface humidity (Granger, 2000; Hashimoto et al., 2008). Hashimoto et al.'s model performed well when validated against a global dataset of 6069 meteorological stations with mean absolute error of 0.25 kPa (Hashimoto et al., 2008). The model performed less well in arid regions with low vegetation cover (leaf area index < 0.5), and in areas near coastlines (within 50 km), where predicted D tended to overestimate observed D.

This current study has two objectives: i) a comparative assessment of the accuracy of D predicted from remote sensing, i.e. from T_{air} and W (following Nieto et al., 2010) and from T_{LST} (following Hashimoto et al., 2008); and ii) a comparative assessment of predictions of FM derived from estimates of D sourced from either remote sensing or gridded weather data. Our work provides a comparison of these remotely sensed methods of D, and a validation of remotely sensed predictions of FM against *in-situ* observations. We used data from MODIS on board the Terra satellite and gridded meteorological data from the SILO database (Jeffrey, Carter, Moodie, & Beswick, 2001). FM predictions were validated against *in-situ* observations of fuel moisture in diverse vegetation types across South East Australia and Southern California.

2. Materials and methods

2.1. Study sites

Remote sensing observations were used to estimate D based on Nieto et al. (2010) and Hashimoto et al. (2008), which were then compared with observations from five flux tower sites: three in South East Australia (Cumberland Plain (Resco de Dios et al., 2015), Tumbarumba (van Gorsel, 2013) and Wombat State Forest (Arndt, 2013)) and two in the Santa Rosa Mountains of Southern California (see Goulden et al., 2012). The three Australian flux tower sites were situated in either eucalypt forest or woodland, while the vegetation at the two Southern Californian Climate Gradient (SCCG) sites was desert chaparral and desert perennials and annuals respectively (Table 1).

In-situ measurements of FM using various methods were conducted at the five flux tower sites, and at an additional 13 locations across South East Australia (Table 1, Fig. 1). These sites were selected to span a wide range of precipitation (588–1404 mm $year^{-1}$) and canopy densities (leaf area index: 0.1–5.7). Vegetation at the Australian sampling sites consisted primarily of woodland, open forest and tall open forest, but also included some heathland.

2.2. Prediction of vapour pressure deficit (D)

2.2.1. Remote sensing

Predictions of D at a daily time-step were made using MODIS products from the Terra satellite, which are available at a 1 km resolution, with overpass time occurring in late morning (approximately 10–11 am local time). The model inputs included T_{LST} from MOD11A1 (collection 5), surface reflectance from MOD09GA and MOD09A1 (collection 5), and W from MOD05_L2 (Table 2). These products are all available at a daily time-step except MOD09A1 which is an 8-day composite product. The MODIS tiles used were h29v12 and h30v12 for South East Australia (for 2013–2014), and h08v05 for California (for 2007–2008). T_{LST} was retrieved using the generalized split-window LST algorithm (Wan, Zhang, Zhang, & Li, 2002). The surface reflectance in seven-bands was derived from MODIS L1-B and corrected for the effects of atmospheric gases and aerosols (Vermote, 2013). W was derived following Gao and Kaufman (2003). These corrected data products are all standard NASA products freely available online (http://reverb.echo.nasa.gov). Data anomalies due to cloud, cloud shadow, cirrus and viewing zenith angles >50.5° were masked using MODIS quality assurance layers. Data was only retained for use in this study where MODIS quality control flags indicated that good quality pixels were produced. For example, for the surface reflectance data (MOD09GA and MOD09A1) we only retained data where the parameter "cloud state" was identified as "clear"; "cloud shadow" was "no"; "cirrus detected" was "none"; and for each individual band, the "data quality" was "highest quality".

D was calculated from remotely sensed estimates of e_s and e_a following Nieto et al. (2010) (D_{TVX}). Estimates of e_s were calculated from T_{air}, which were in turn calculated using the Temperature-Vegetation Index (TVX) method. The TVX method assumes that T_{LST} over a fully vegetated canopy approaches T_{air}. Thus, a linear relationship between the remotely sensed vegetation index NDVI and T_{LST} is used to estimate T_{air}, by extrapolating this relationship to a fully vegetated canopy ($NDVI_{max}$) (Goetz, 1997; Nieto, Sandholt, Aguado, Chuvieco, & Stisen, 2011; Prihodko & Goward, 1997; Stisen, Sandholt, Norgaard, Fensholt, & Eklundh, 2007). Here, we calculated $NDVI_{max}$ following Nieto et al. (2011) for each of the five flux tower sites. Values ranged from 0.23, for the Sonoran desert, to 0.80 for the Tumbarumba forest. NDVI was calculated from 8-day composite surface reflectance data (MOD09A1)

Table 1
Description of fuel moisture sampling sites.

Site number	Site name	Vegetation	Location (Latitude °N; longitude °E)	Elevation (m)	Mean annual rainfall (mm year^{-1})	Leaf area index[a]
Flux tower sites						
7	Cumberland Plain Woodland (calibration site)	Eucalyptus and Melaleuca woodland	−33.6153; 150.7237	25	801	1.9
9	Wombat Forest[c]	Eucalypt tall open forest	−37.4222; 144.0944	713	871	4.8
15	Tumbarumba Forest[c]	Eucalypt tall open forest	−35.6566; 148.1517	1200	1000	5.2
1	SCCG Sonoran Desert[b]	Desert perennials and annuals	33.6518; −116. 3721	275	129	0.1
2	SCCG Desert Chaparral[b]	Desert shrubland	33.6100; −116.4502	1300	313	0.3
Additional South East Australian sites						
3	Chiltern Box National Park[d]	Eucalypt open forest	−36.1302; 146.6199	265	588	1.2
4	Chiltern Pilot National Park[d]	Eucalypt open forest	−36.2704; 146.6531	435	588	1.1
5	Mellong[d]	Heathland	−33.1302; 150.6995	315	594	1.8
6	Mt Granya National Park[d]	Eucalypt open forest	−36.1387; 147.3322	530	699	1.2
8	Blue Mountains National Park, site A[d]	Eucalypt woodland	−33.6107; 150.6384	192	833	2.0
10	Burragorang State Recreation Area[d]	Eucalypt woodland	−34.0302; 150.5053	439	886	5.3
11	Bago State Forest[d]	Eucalypt tall open forest	−35.6468; 148.1483	1200	943	5.6
12	Bemm State Forest[d]	Eucalypt tall open forest	−37.6050; 148.9056	161	975	3.6
13	Club Terrace State Forest[d]	Warm temperate rainforest	−37.6516; 148.8167	154	975	4.1
14	Tamboon State Forest[d]	Eucalypt tall open forest	−37.5679; 149.1088	122	975	2.9
16	Blue Mountains National Park, site B[d]	Eucalypt woodland	−33.7447; 150.3900	837	1300	5.7
17	Kinglake National Park[d]	Eucalypt tall open forest	−37.4766; 145.2334	528	1359	3.8
18	Megalong[d]	Eucalypt woodland	−33.6895; 150.2342	747	1404	1.6

SCCG = Southern Californian Climate Gradient.
[a] Leaf area index calculated over a one year period, coinciding with the sampling period, from MODIS 8-day composite dataset MOD15A2 (collection 5), available online from: http://reverb.echo.nasa.gov.
[b] Data from Goulden et al. (2012).
[c] Data from Ozflux (http://www.ozflux.org.au/monitoringsites/index.html).
[d] Rainfall data is from the nearest weather station, located within 30 km of the sampling site, data obtained from the Australian Bureau of Meteorology (http://www.bom.gov.au).

following equation 4 (Tucker, 1979):

$$\mathrm{NDVI} = \frac{\mathrm{Band\,2} - \mathrm{Band\,1}}{\mathrm{Band\,2} + \mathrm{Band\,1}} \quad (4)$$

where Band 2 and Band 1 measure near infrared and red wavelengths respectively. A 9 by 9 pixel window centred on the study site was used to regress NDVI against daily T_{LST} and subsequently calculate T_{air} for the central pixel. Given the Terra satellite overpass time was late-morning, these regressions were specific to that time of day.

Estimates of e_a were calculated from W following Eq. (5)

$$e_a = g\frac{W(\lambda+1)}{\delta} \quad (5)$$

where δ is the ratio of the specific gas constants of water vapour and dry air (0.622); g is the acceleration due to gravity; and λ is the exponent of the power law that describes the decrease in moisture with altitude through the atmospheric profile. The value of λ changes with latitude and season, and was calculated following Smith (1966) for the Northern

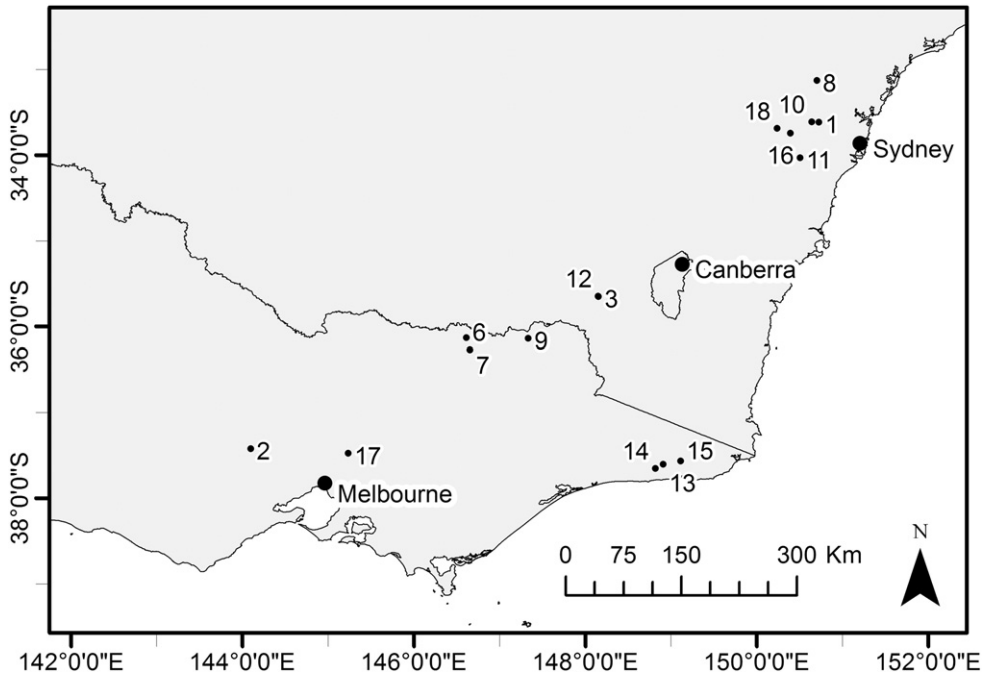

Fig. 1. Location of fuel sampling sites across South East Australia. Site labels correspond to Table 1.

Table 2
Summary of methods used to estimate meteorological variables.

Variable	Abbreviation	Approach	Datasets
Land surface temperature	T_{LST}	MODIS product (Wan & Dozier, 1996)	MOD11
Air temperature	T_{air}	Calculated using TVX method (Goward et al., 1994; Nemani & Running, 1989)	MOD09, MOD11
Saturation vapour pressure	e_s	Calculated either from T_{air} or T_{LST}.	
Actual vapour pressure	e_a	Derived from W (Prince, Goetz, Dubayah, Czajkowski, & Thawley, 1998)	MOD05
Vapour pressure deficit	D_{TVX}	From e_s (derived from T_{air}) and e_a (Nieto et al., 2010)	MOD09, MOD11, MOD05
	D_{LST}	Empirical model based on e_s (derived from T_{LST}) (Hashimoto et al., 2008)	MOD11
	D_{SILO}	Interpolated weather station data (Jeffrey et al., 2001)	SILO climate data

TVX = temperature vegetation index; W = precipitable water in the atmosphere.

hemisphere sites, and following Viswanadham (1981) for the Southern hemisphere sites.

D was also calculated following Hashimoto et al. (2008) (D_{LST}) from an empirical relationship between e_s, calculated using T_{LST}, rather than T_{air}, and ground-based observations of D:

$$D_{LST} = 0.353 * e_s + 0.154. \quad (6)$$

2.2.2. In-situ observations

Each of the MODIS derived meteorological estimates, T_{LST}, e_a, D_{TVX} and D_{LST}, was averaged across a 3 by 3 pixel window centred over each of the five flux tower sites. This window size was selected to average-out spatial heterogeneity; a similar approach was used previously to predict fuel moisture from remotely sensed data (Caccamo, Chisholm, Bradstock, & Puotinen, 2011). Our MODIS-based estimates were validated against the corresponding mean daytime observations from the flux tower sites. These comparisons were made for June 2013–May 2014 at the South-East Australian sites; over 2007 at the SCCG Desert Chaparral site; and over 2008 at the SCCG Sonoran Desert site. Half-hourly observations of T_{air} and RH were used to calculate e_s, e_a and D following Eqs. (1)–(3). Measurements of T_{air} and RH were made using HMP probes (Vaisala, Helsinki, FI) mounted on towers 5–10 m above the canopy.

2.2.3. Gridded meteorological observations

Gridded daily weather data from the SILO database (http://www.longpaddock.qld.gov.au/silo/index.html) was used to estimate D (D_{SILO}) on a spatially explicit basis. SILO estimates are based on interpolation of weather station records across Australia on a 0.05° grid (Jeffrey et al., 2001). Daily D was estimated from maximum T_{air} and RH at the time of maximum T_a, following Eqs. (1)–(3). D_{SILO} was estimated for the South East Australian sites during April 2013–December 2014.

2.3. In-situ observations of dead fine fuel moisture content (FM)

In-situ FM was measured in two ways: with automated sensors and with manual measurements. Automated measurements were made at the Cumberland Plain and Southern Californian flux tower sites. Automated FM was monitored every 30–60 min with a fuel moisture sensor connected to a data logger (CS505; Campbell Scientific Inc., Logan, UT, USA). The sensor uses Time Domain Reflectometry (TDR) to measure the moisture content of a 10-hour (13 mm diameter) Ponderosa Pine stick. At the Cumberland Plain site three fuel moisture sensors were installed facing north at 30 cm above ground and *ca.* 100 m apart, while at the Californian sites 1–2 sensors were installed at ground level. Data from the fuel moisture sensors at each site were averaged to obtain site level estimates of FM (Resco de Dios et al., 2015). Dead fine fuel moisture was monitored over 24 months at the Cumberland Plain site (2013–2014), and over 12 months at each of the two Californian sites (2007 for the Chaparral and 2008 for Sonoran Desert).

Manual FM measurements were collected by periodic destructive sampling at 16 sites in South East Australia, including the three flux tower sites (Table 1, Fig. 1). Two types of fuel were sampled: suspended 10-hour fuel (small sticks, 6.35–25 mm diameter) and suspended 1-hour fine fuel (litter < 6.35 mm). Suspended fuels are those which are not in contact with the soil, e.g. fuels that are detached, but hanging from plants. Five tins of each fuel type were harvested at three locations at the Cumberland Plain site, corresponding with the three fuel moisture sensors located around the flux tower. We did not observe systematic intra-site variation (authors' unpublished data), and therefore averaged the values from all of the tins to obtain a single site value. Between 5 and 10 tins of each fuel type were harvested at the remaining sites, depending on site variability, and all tins were averaged to obtain a single site value. Approximately 40 g of dried 10-hour fuel and 10 g of dried fine fuel were collected per tin. Samples were oven-dried at 105 °C for 48 h. Sampling at the three Australian flux tower sites occurred over a twelve month period, every 2–4 weeks at the Cumberland Plain site and 4–6 weeks at Tumbarumba and Wombat. Sampling at the remaining sites occurred approximately monthly during a four month period in the spring and summer fire season. All of the South-East Australia sampling was done in 2013–2014.

2.4. FM model

FM was predicted from D using the FM_D model of Resco de Dios et al. (2015):

$$FM = FM_0 + FM_1 e^{(-mD)} \quad (7)$$

where FM_0 is minimum FM, $FM_0 + FM_1$ is the FM when D is zero, and m is the rate of change in FM with D. Resco de Dios et al. (2015) proposed estimates for FM_0, FM_1 and m to be used in subsequent estimates of FM, but we recalibrated the model at the Cumberland Plain flux tower site using the larger spatial resolution of the remotely sensed (9 km^2) and SILO estimates of D (25 km^2). The parameters FM_0, FM_1 and m were obtained by fitting the model with non-linear least squares (R Development Core Team, 2014). We used D from the model that had the greatest accuracy when compared with ground-based observations of D, i.e. D_{TVX} or D_{LST}, not both.

2.4.1. Calibration data

The FM_D model was calibrated using both remotely sensed estimates of D and D_{SILO}, and a subset of the *in-situ* FM observations: i.e. six months of fuel moisture sensor data at the Cumberland Plain site. We chose July–December, 2013 for the calibration period since the period included a wide range of D. FM over the calibration period ranged from 5.6–47%. The observations used for calibration were independent of those used to develop and test the FM_D model of Resco de Dios et al. (2015). Given that daily minimum values of FM are critical in determining fire risk, the model was calibrated with minimum, daytime records of the fuel moisture sensors. We excluded days of significant rainfall (>2 mm).

2.4.2. Validation data

The calibrated FM_D model derived from remote sensing was tested with fuel moisture sensor observations collected at Cumberland Plain (April–June 2013 and January–December 2014), SCCG Chaparral

(January–December 2007) and the Sonoran Desert (January–December 2008). The model was further tested against fuel moisture measurements from destructive sampling at the 16 South East Australia sites. The calibrated model based on D_{SILO} was tested using the fuel moisture observations from the Cumberland Plain and the destructive sampling across South East Australia.

Given substantial gaps in the MODIS daily time-series data (MOD11A1 and MOD09GA), we compared observed FM with predictions from the MODIS based model both on the day of sampling, if available, or on the day immediately prior to sampling, otherwise data was excluded. We separately examined the performance of the FM_D models when fuel moisture values were <30%, which is around fibre saturation point (Berry & Roderick, 2005). We also examined the performance of the model when observed values were <20%, given that lower fuel moisture values are of greater importance for determining fire risk.

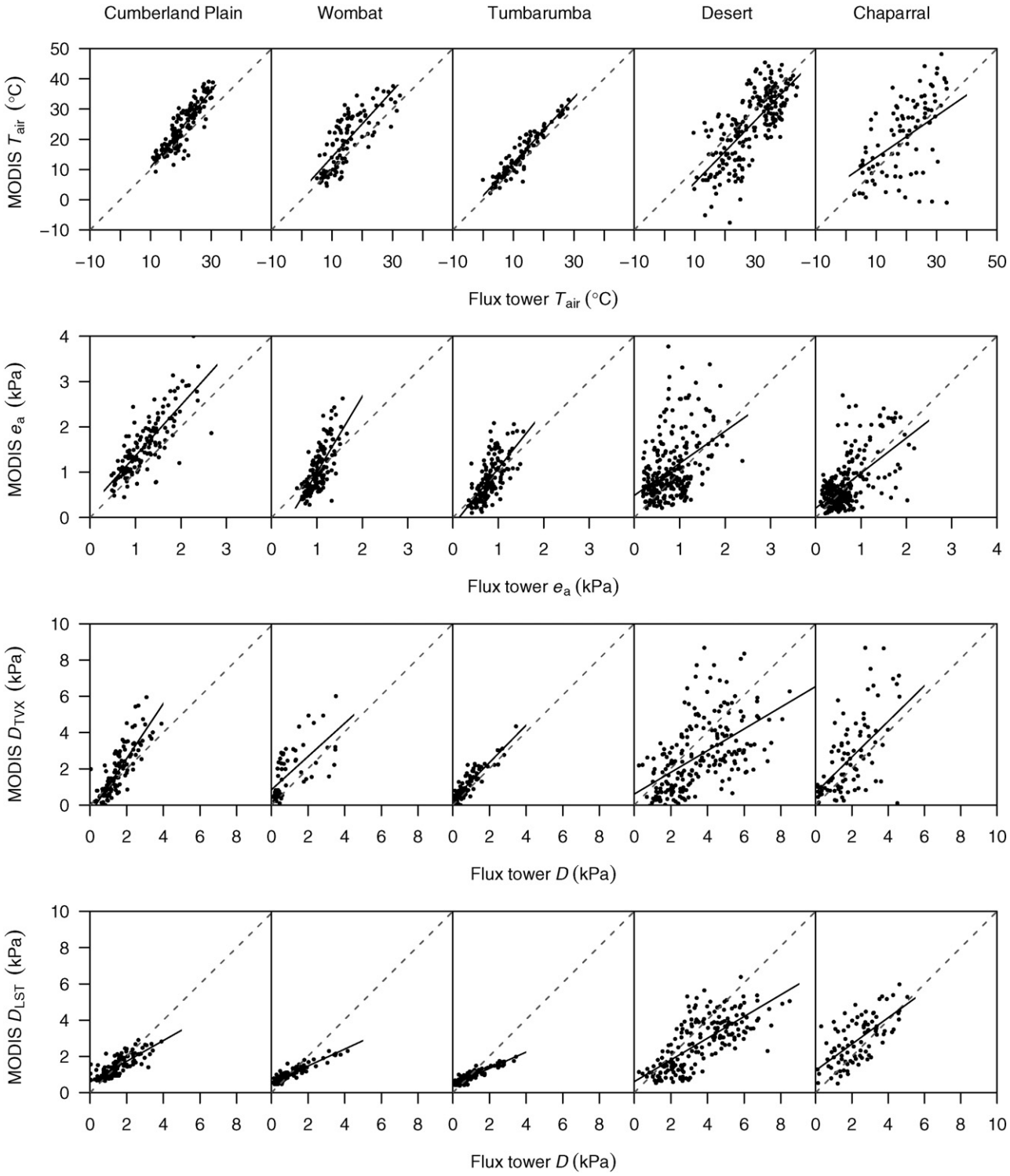

Fig. 2. Linear regressions of observed mean, daytime meteorological variables against remotely sensed values (solid line). Data are averaged from a 3 by 3 pixel window (i.e. 9 km^2) centred over the flux tower. Also shown is the 1:1 line (dashed line). T_{air} is air temperature, e_a is actual vapour pressure, D is vapour pressure deficit, D_{TVX} is D predicted following Nieto et al. (2010) and D_{LST} is D predicted following Hashimoto et al. (2008).

The accuracy of predictions against observations was assessed for each model using the mean absolute error (MAE), mean biased error (MBE) and the r^2 of the regression of predicted compared to observed values. The MAE and MBE are expressed as absolute values in the unit of measurement, i.e. in kPa for D and in percentage for FM. All analyses were done in R (R Development Core Team, 2014) using the raster (Hijmans, 2013) and sirad (Bojanowski, 2013) packages.

3. Results

3.1. Validation of remotely sensed vapour pressure deficit

Both MODIS D_{TVX} and D_{LST} were good predictors of *in-situ* D, especially at the forest and woodland sites (Fig. 2, Table 3). D_{TVX} tended to over-predict D, with MBE ranging from −0.85 to 0.74 kPa, while D_{LST} tended to under-predict D, particularly at the higher range of D, with MBE ranging from −0.83 to 0.60. D_{LST} consistently had the lowest MAE, ranging from 0.30 to 1.16 kPa, compared to D_{TVX}, where MAE ranged from 0.37 to 1.62 kPa. D_{LST} also had either a similar or stronger relationship with observed D, with r^2 ranging from 0.45 to 0.86, compared to D_{TVX}, where r^2 ranged from 0.19 to 0.89. D_{LST} was subsequently used for calibrating the FM_D model.

Error in the prediction of *in-situ* D using D_{TVX} reflected uncertainties in both T_{air} and e_a (Fig. 2, Table 3). In particular e_a tended to have a weaker relationship with *in-situ* values, with r^2 ranging from 0.19 to 0.64, compared to T_{air}, with r^2 ranging from 0.19 to 0.89.

3.2. Validation of dead fine fuel moisture content model

Calibration of the FM_D model with D from remotely sensed data (D_{LST}) and gridded meteorological data (D_{SILO}) gave:

$$FM = 7.86 + 140.94\, e^{(-3.73 D_{LST})} \quad (8)$$

$$FM = 6.79 + 27.43 e^{(-1.05 D_{SILO})}. \quad (9)$$

The shape and strength of the relationship between FM and D was similar for both calculations of D, with $r^2 = 0.66$ for D_{LST}, and $r^2 = 0.70$ for D_{SILO} (Fig. 3).

Performance of the FM_D model was consistent across the different vegetation types (Table 4, Fig. 4). A comparison of FM predicted from D_{LST} observations (Eq. (8)) against the *in-situ* FM observations from sensor data gave a MAE ranging from 2.3 to 2.9%, with the model tending to under-predict FM: MBE ranged from −1.3 to −2.0%. Note, these errors represent absolute values of FM, with FM units expressed as a percentage. Observed FM in the validation datasets ranged from 5.3 to 49.3% across the flux tower sites. Predictions based on D_{LST} compared with the destructively harvested samples at the 16 South East Australia sites yielded a MAE of 3.9% for the 10-hour fuels, and 2.3% for the 1-hour fuels. The observed range of FM was 4.5–71% across the harvested fuels. The model performance increased for all fuel types when moisture content was <30%. This was particularly evident for 1-hour suspended fuel (destructively sampled) where moisture content values up to 71% moisture were observed (Fig. 4f). The MAE of 1-hour suspended FM predicted from D_{SILO} decreased from 4.7% to 3.2% for moisture content <30%, and to 2.2% for moisture content <20%.

The performance of the FM_D model was similar when the model was calibrated with D_{LST} or with D_{SILO} (Table 4, Fig. 4). For example at the Cumberland Plain woodland site the MAE of FM sensor data was 2.9% when predicted from D_{LST} (Fig. 4a) and 2.0% when predicted from D_{SILO} (Fig. 4b). The MAE of destructively harvested FM was similar or higher when the model was calibrated with D_{SILO} compared to D_{LST}. Predictions for destructively harvested 10-hour fuel for FM < 30% resulted in a MAE 3.9% when using D_{LST} compared with 4.2% when using D_{SILO} (Fig. 4c–d). Similarly, the MAE of destructively harvested 1-hour fuel was 2.1% when D_{LST} was used, and 3.2% when D_{SILO} was used (Fig. 4e–f). However, there was a substantial difference in the number of days D_{LST} and D_{SILO} could be calculated. For example, for the validation of the model with fuel moisture sensor data, D_{SILO} was available for every day across the validation period ($n = 341$), whereas D_{LST} was available for less than half of the days ($n = 153$).

4. Discussion

Predictions of D based on Nieto et al.'s (2010) and Hashimoto et al.'s (2008) approaches both agreed favourably with the *in-situ* observations, with the predictions based on D_{LST} alone yielding comparatively lower MAEs. The FM predictions calculated with Resco de Dios et al.'s (2015) FM_D model and the D_{LST} remote sensing approach performed well when compared with *in-situ* observations; this agreement held across a range of vegetation types in South East Australia and Southern California. Predictions based on gridded meteorological data (D_{SILO}) also performed well when compared with *in-situ* observations. Both approaches therefore offer potential for further development and subsequent operational application to predict dead fine fuel moisture at large spatial scales.

4.1. Performance of remotely sensed vapour pressure deficit models

The modelling of remotely sensed meteorological variables based on T_{LST} following Nieto et al. (2010) and D following Hashimoto et al. (2008) performed similarly well (Table 3, Fig. 2). Both T_{air} and D_{LST} predictions performed better at sites with relatively high LAI, i.e. the forest and woodland sites. This was consistent with the findings of Hashimoto et al. (2008), who similarly found the link between T_{LST} and D deviated in regions where LAI was less than 0.5. Indeed, T_{LST} is often under-predicted in arid and semi-arid areas (Wan et al., 2002). Thus, in our study the poorer performance of D_{TVX} compared to D_{LST} was due to e_a, which was less precise than T_{air}. This is consistent with Nieto et al. (2010) who also found poorer prediction of e_a when modelled on a daily-time-step, due to the variability of e_a in the atmosphere during the day. Additionally, e_a performance may have been affected by a lower accuracy of the MOD05 product over parts of Australia, which is reportedly due to iron-rich soils affecting spectral reflectance (Lyapustin et al., 2014). Given this, the strategy of modelling D based

Table 3
Validation of MODIS meteorological variables against corresponding on-ground observations measured over one year at each of the flux tower sites. On-ground observations are mean, daytime value.

Variable	MAE	MBE	r^2	n
T_{air}				
Cumberland Plain Woodland	4.24 °C	3.54 °C	0.78	147
Wombat Forest	5.58 °C	4.56 °C	0.63	107
Tumbarumba Forest	2.72 °C	2.30 °C	0.89	103
SCCG Sonoran Desert	6.74 °C	−3.88 °C	0.55	214
SCCG Desert Chaparral	8.82 °C	1.00 °C	0.19	95
e_a				
Cumberland Plain Woodland	0.45 kPa	0.39 kPa	0.64	141
Wombat Forest	0.28 kPa	0.02 kPa	0.54	148
Tumbarumba Forest	0.26 kPa	0.03 kPa	0.47	164
SCCG Sonoran Desert	0.48 kPa	0.25 kPa	0.19	257
SCCG Desert Chaparral	0.33 kPa	0.06 kPa	0.34	290
D_{TVX}				
Cumberland Plain Woodland	0.66 kPa	0.30 kPa	0.69	127
Wombat Forest	0.97 kPa	0.74 kPa	0.43	60
Tumbarumba Forest	0.37 kPa	0.30 kPa	0.81	96
SCCG Sonoran Desert	1.62 kPa	−0.85 kPa	0.28	212
SCCG Desert Chaparral	1.45 kPa	0.63 kPa	0.26	94
D_{LST}				
Cumberland Plain Woodland	0.36 kPa	−0.03 kPa	0.62	136
Wombat Forest	0.36 kPa	0.02 kPa	0.85	120
Tumbarumba Forest	0.30 kPa	−0.06 kPa	0.86	138
SCCG Sonoran Desert	1.16 kPa	−0.83 kPa	0.53	197
SCCG Desert Chaparral	0.92 kPa	0.60 kPa	0.45	91

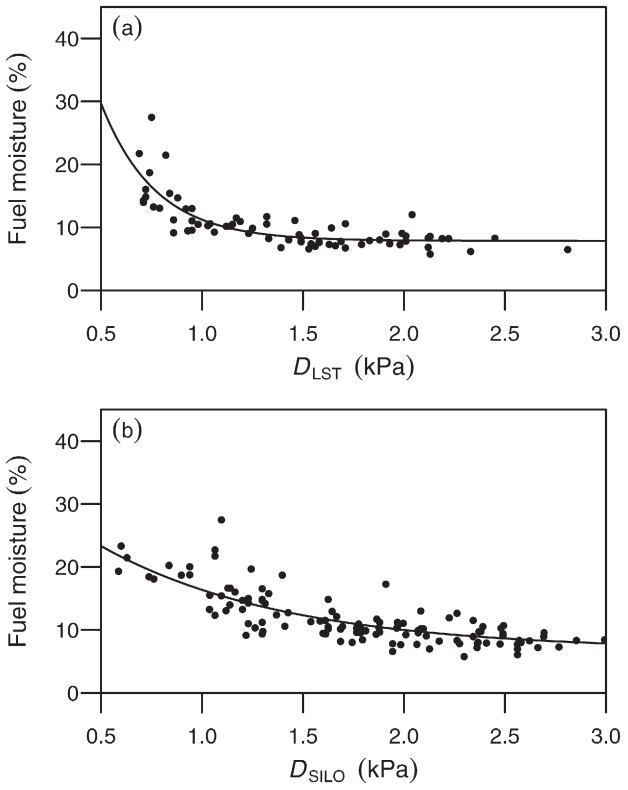

Fig. 3. Models of minimum daytime dead fine fuel moisture content, calibrated, at the Cumberland Plain flux tower site, separately with (a) D_{LST} and (b) D_{SILO}. The model equations are: (a) $FM = 7.86 + 104.94 * e^{(-3.73 D_{LST})}$, $r^2 = 0.66$, $n = 71$; (b) $FM = 6.79 + 27.43 * e^{(-1.05 D_{SILO})}$, $r^2 = 0.70$, $n = 165$.

solely on T_{LST} (i.e. following the method of Hashimoto et al. (2008)) may be preferable in landscapes dominated by forest and woodland, where LAI is relatively high.

Given that remotely sensed D, which represents an instantaneous prediction, was regressed against mean, daytime flux tower D, this difference in temporal resolution may have affected model performance. However, the meteorological variables predicted by remotely sensed data were neither consistently over- nor under-predicted (Fig. 2, Table 3). This suggests that D modelled from MODIS Terra data is predicting D over a wider temporal range than just at the satellite overpass time (late-morning). This is perhaps related to the relatively large spatial resolution used in this study (9 km^2), with mean, daytime D observed at the flux tower providing a better integration of D across this area than any single, instantaneous, observation of D.

4.2. Performance of FM_D model

The good performance of the FM_D model, irrespective of being calibrated with D_{LST} or with D_{SILO} (Table 4, Fig. 4), indicates that prediction of FM is viable at regional to sub-continental scales from either remotely sensed data or gridded meteorological data. The performance of the FM_D model was similar to that reported in Resco de Dios et al. (2015). The MAE of FM in our study was less than 2.9%, when compared with fuel moisture sensor data (Table 4), whereas Resco de Dios et al. (2015) reported a MAE of 3.7% across several sites (although sample size was smaller in the current study). The MAE we found was similar to the reported instrument error for the fuel moisture sensors of 3.1% (Resco de Dios et al., 2015), indicating the model is robust across a range of species and canopy densities. The model, though calibrated on observations at the Australian woodland site, also performed well for the Southern Californian sites, which had low LAI and where modelled D was less accurate. This performance of the FM_D model may have been due to the relatively low values of moisture content observed at these sites, given that the FM_D model performed best when moisture contents were low (Fig. 4).

The poorer performance of the FM_D model with wetter fuels is consistent with previous reports, e.g. Matthews, McCaw, Neal, and Smith (2007) and Catchpole et al. (2001). The reduced performance of FM models at higher moisture content is attributable to the greater variability in moisture content of wet fuels, as evidenced by the higher standard error associated with destructively harvested fuels (Fig. 4c–f). This does not limit the potential for practical application of the FM_D model, given that model performance was only substantially reduced for the moisture content range above 30% (Fig. 4), which is above fibre saturation point (Berry & Roderick, 2005).

4.3. Application of the FM_D model

The calibrated FM_D models presented here are suitable for use at spatial scales relevant to operational fire management. The MAE of the calibrated models was less than 5.0% across a range of fuel classes and vegetation types, which was lower than for other models widely used

Table 4
Validation of the FM_D model with observations from fuel moisture sensors and from destructively harvested fuel. 10-hour fuel (CS505) is FM measured with a fuel moisture sensor inserted into a 19 mm ponderosa pine dowel. 10-hour fuel is suspended small sticks, 6.35–25 mm diameter. 1-hour fuel is suspended litter <6.35 mm. Days with >2 mm rain were excluded from analysis.

Fuel type	Site	D_{LST}				D_{SILO}			
		MAE (%)	MBE (%)	r^2	n	MAE (%)	MBE (%)	r^2	n
10-hour (CS505)									
Full dataset	Cumberland Plain	2.9	−1.4	0.29	153	2.0	−0.7	0.57	341
	SCCG Desert	2.3	−1.3	0.22	245	NA	NA	NA	NA
	SCCG Chaparral	2.6	−2.0	0.09	88	NA	NA	NA	NA
FM < 30%	Cumberland Plain	2.8	−1.3	0.31	152	2.0	−0.7	0.59	340
	SCCG Desert	2.0	−1.1	0.36	243	NA	NA	NA	NA
	SCCG Chaparral	2.2	−1.5	0.15	87	NA	NA	NA	NA
FM < 20%	Cumberland Plain	2.4	−0.8	0.34	145	1.7	−0.4	0.57	323
	SCCG Desert	1.9	−0.9	0.36	238	NA	NA	NA	NA
	SCCG Chaparral	2.0	−1.4	0.20	86	NA	NA	NA	NA
10-hour									
Full dataset	SE Australian sites	3.9	−3.3	0.34	67	4.2	−2.4	0.46	92
FM < 30%	SE Australian sites	3.9	−3.3	0.34	67	3.8	−1.9	0.28	88
FM < 20%	SE Australian sites	3.2	−2.6	0.23	58	2.8	−0.6	0.23	73
1-hour									
Full dataset	SE Australian sites	2.3	−1.0	0.63	67	4.7	−3.9	0.46	92
FM < 30%	SE Australian sites	2.1	−0.8	0.58	66	3.2	−2.5	0.33	88
FM < 20%	SE Australian sites	2.1	−0.8	0.41	64	2.2	−1.3	0.43	78

in fire danger indices (Resco de Dios et al., 2015). Given that the FM_D models performed similarly well when evaluated across a range of vegetation types (LAI ranging from 0.1 to 5.7, Table 1) and moisture contents, site-specific calibrations of the FM_D model for different fuel types or canopy densities are not required.

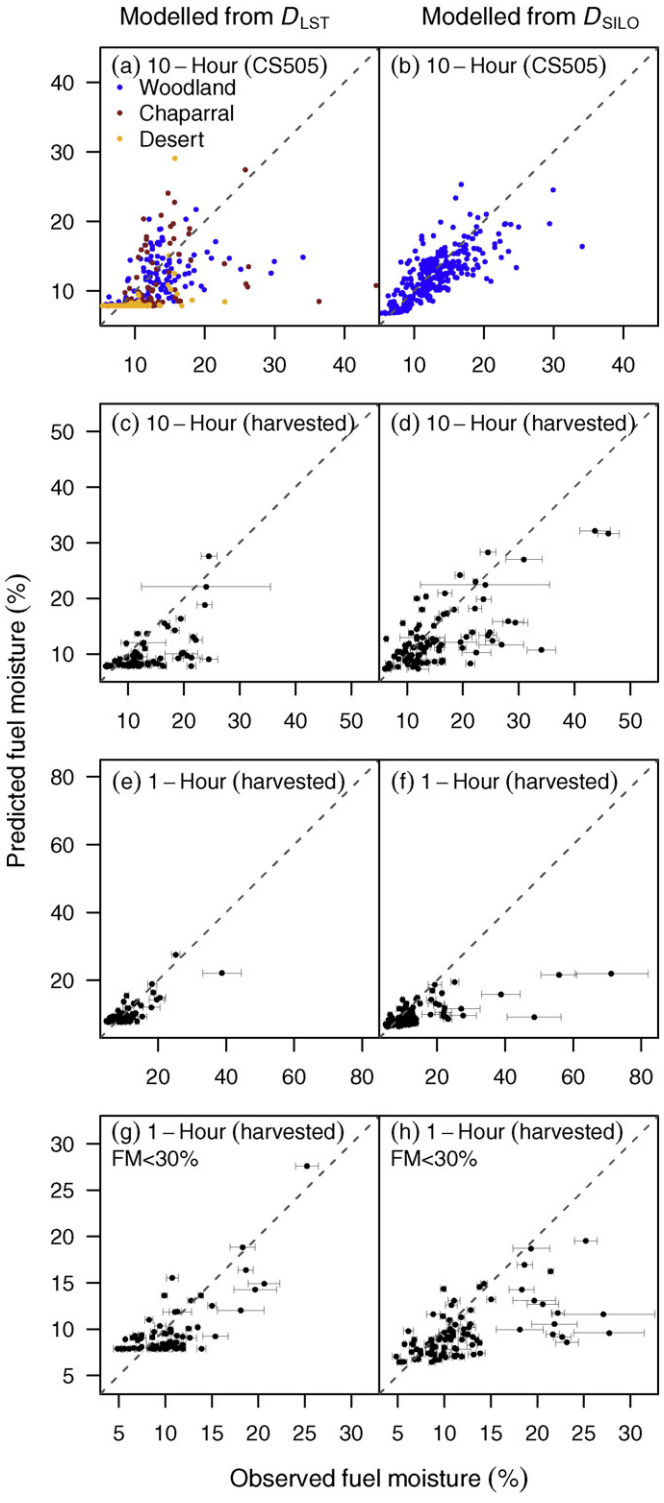

Fig. 4. Observed and predicted values of dead fine fuel moisture content (FM). Fuel types are: 10-hour fuel from fuel moisture sensors (CS505) (a–b); destructively harvested 10-hour suspended fuel (c–d); and destructively harvested 1-hour suspended fuel (e–f). FM was predicted from vapour pressure deficit (D) from either remotely sensed data (D_{LST}) or from spatially interpolated weather station data (D_{SILO}), the latter for the South East Australian sites only. Fuel moisture sensor data is from the Cumberland Plain Woodland, SCCG Chaparral and SCCG Sonoran Desert flux tower sites, while destructively harvested fuel is from 16 sites across South East Australia. Destructively harvested fuels represent the mean ± 1 SE. The scale for the y- and x-axes may vary between panels.

The FM_D model based on D_{LST} can be easily applied across a range of forest and woodland environments given the wide availability of MODIS data. The primary disadvantage in using remotely sensed D is gaps in daily MODIS data products MOD11A1 and MOD09GA, primarily due to cloud cover. For example, 24% of MOD11A1 data was unavailable at the Cumberland Plain woodland site over the validation period (Table 4). Further, there was an additional Southern Californian flux tower site which was not included in this study, but that was included in the original Resco de Dios et al. (2015) study, because no MODIS data was available over the period of fuel moisture sampling. These cloudy days were not correlated with increased humidity, and thus higher fuel moisture (data not shown). While MODIS 8-day data could overcome this problem to some extent, fine fuels respond to atmospheric conditions which can change substantially over an 8-day period. This is in contrast to live fuels, which respond more gradually to changes in atmospheric and soil moisture conditions, and are often monitored once every 8 or 16 days (Caccamo et al., 2012; Chuvieco et al., 2004; Peterson, Roberts, & Dennison, 2008; Yebra et al., 2013). Use of a geostationary satellite rather than a polar orbiting satellite may also have potential for partially overcoming data gaps, due to its higher temporal resolution (one hour or less). The Japanese Multi-functional Transport Satellite (MTSAT) and the recently launched Himawari-8 have recently been shown to model T_{LST} with similar accuracy to MODIS, provided that cloud contamination of images can be accurately assessed (Oyoshi, Akatsuka, Takeuchi, & Sobue, 2014). Use of a geostationary satellite with hourly or better temporal resolution would also provide more accurate measurements of minimum FM, which generally occurs in the afternoon, while the MODIS Terra overpass time is late morning, and the MODIS Aqua operpass time is a single time in early afternoon.

Spatially gridded meteorological datasets may overcome the limitations of remotely sensed D and thus be preferable for operational use in monitoring FM, particularly in the fire season. Additionally, there is the potential for predicting D and resultant FM from forecasts by meteorological agencies in near real time, for example the Australian Bureau of Meteorology's Numerical Weather Prediction System (http://www.bom.gov.au/nwp/doc/access/NWPData.shtml). Such a capability may assist in anticipating and predicting the potential for wildfires, and may also be useful for planning prescribed burns. In locations where gridded meteorological datasets are less reliable, satellite datasets could be merged with meteorological data, to improve estimation of D. For example, remotely sensed thermal infrared data can be used to inform the spatial interpolation of *in-situ* weather station data (Wu & Li, 2013).

5. Conclusions

We have shown that the moisture content of suspended dead fine fuels can be monitored and forecast across large spatial areas using a simple model based on D. This model can be applied across a range of vegetation types without the need for site-specific calibration. Although the FM_D model performed well across a range of canopy densities, we recommend caution if using remotely sensed estimates of D in areas with low LAI, due to the tendency of remotely sensed T_{LST} to be under-predicted in these areas.

Acknowledgements

We would like to thank R. Gibson, M. Chick, D. Spencer, S. Khanal, A. Boer-Cueva, L. Serrano-Grijalva, D. Bridgman, and C. Beattie for their invaluable assistance in collecting fuel moisture data. This project was funded by Victorian Department of Environment, Land, Water and Planning via the Bushfire Cooperative Research Centre, grants from the US Department of Energy and the National Aeronautics and Space Administration to MLG, the Education Investment Fund, the Hawkesbury

Institute for the Environment and a Ramón y Cajal Fellowship to VRD (RYC-2012-10970). MODIS data products are courtesy of the online Data Pool at the NASA Land Processed Distributed Archive Centre (LP DAAC), USGS/Earth Resources Observation and Science (EROS) Center, Sioux Falls, South Dakota (https://lpdaac.usgs.gov/data_access).

References

Arndt, S.K. (2013). Wombat State Forest OzFlux-tower site OzFlux: Australian and New Zealand Flux Research and Monitoring hdl: 102.100.100/14237.

Berry, S.L., & Roderick, M.L. (2005). Plant–water relations and the fibre saturation point. *New Phytologist*, *168*, 25–37.

Bojanowski, J.S. (2013). sirad: Functions for calculating daily solar radiation and evapotranspiration. R package version 2.0-7. http://CRAN.R_project.org/package=sirad.

Bowyer, P., & Danson, F.M. (2004). Sensitivity of spectral reflectance to variation in live fuel moisture content at leaf and canopy level. *Remote Sensing of Environment*, *92*, 297–308.

Bradshaw, L., Deeming, J., Burgan, R.E., & Cohen, J. (1983). *The 1978 National Fire-Danger Rating System: Technical documentation, GTR-INT-169.* Ogden, UT: USDA, Forest Service.

Caccamo, G., Chisholm, L.A., Bradstock, R.A., & Puotinen, M.L. (2011). Assessing the sensitivity of MODIS to monitor drought in high biomass ecosystems. *Remote Sensing of Environment*, *115*, 2626–2639.

Caccamo, G., Chisholm, L.A., Bradstock, R.A., Puotinen, M.L., & Pippen, B.G. (2012). Monitoring live fuel moisture content of heathland, shrubland and sclerophyll forest in south-eastern Australia using MODIS data. *International Journal of Wildland Fire*, *21*, 257–269.

Catchpole, E.A., Catchpole, W.R., Viney, N.R., McCaw, W.L., & Marsden-Smedley, J.B. (2001). Estimating fuel response time and predicting fuel moisture content from field data. *International Journal of Wildland Fire*, *10*, 215–222.

Ceccato, P., Flasse, S., & Gregoire, J. (2002). Designing a spectral index theory to estimate vegetation water content from remote sensing data: Part 2. Validation and applications. *Remote Sensing of Environment*, *82*, 198–207.

Chuvieco, E., Cocero, D., Riano, D., Martin, P., Martinez-Vega, J., de la Riva, J., & Perez, F. (2004). Combining NDVI and surface temperature for the estimation of live fuel moisture content in forest fire danger rating. *Remote Sensing of Environment*, *92*, 322–331.

Gao, B.C., & Kaufman, Y.J. (2003). Water vapor retrievals using moderate resolution imaging spectroradiometer (MODIS) near-infrared channels. *Journal of Geophysical Research-Atmospheres*, *108*.

Goetz, S.J. (1997). Multi-sensor analysis of NDVI, surface temperature and biophysical variables at a mixed grassland site. *International Journal of Remote Sensing*, *18*, 71–94.

Goulden, M.L., Anderson, R.G., Bales, R.C., Kelly, A.E., Meadows, M., & Winston, G.C. (2012). Evapotranspiration along an elevation gradient in California's Sierra Nevada. *Journal of Geophysical Research – Biogeosciences*, *117*.

Goward, S.N., Waring, R.H., Dye, D.G., & Yang, J.L. (1994). Ecological remote-sensing at OTTER — Satellite macroscale observations. *Ecological Applications*, *4*, 322–343.

Granger, R.J. (2000). Satellite-derived estimates of evapotranspiration in the Gediz basin. *Journal of Hydrology*, *229*, 70–76.

Hashimoto, H., Dungan, J.L., White, M.A., Yang, F., Michaelis, A.R., Running, S.W., & Nemani, R.R. (2008). Satellite-based estimation of surface vapor pressure deficits using MODIS land surface temperature data. *Remote Sensing of Environment*, *112*, 142–155.

Hijmans, R.J. (2013). Raster: Geographic data analysis and modeling. R package version 2.1-62/r2833. http://R-Forge.R-project.org/projects/raster/.

Jeffrey, S.J., Carter, J.O., Moodie, K.M., & Beswick, A.R. (2001). Using spatial interpolation to construct a comprehensive archive of Australian climate data. *Environmental Modelling & Software*, *16*, 309–330.

Keetch, J.J., & Byram, G.M. (1968). A drought factor index for forest fire control. *USDA Forest Service, Southeastern Forest Experiment Station, Research Paper SE-38 (Asheville, NC)*.

Lyapustin, A., Alexander, M.J., Ott, L., Molod, A., Holben, B., Susskind, J., & Wang, Y. (2014). Observation of mountain lee waves with MODIS NIR column water vapor. *Geophysical Research Letters*, *41*(2), 710–716.

Matthews, S. (2013). Dead fuel moisture research: 1991–2012. *International Journal of Wildland Fire*, *23*(1).

Matthews, S., McCaw, W.L., Neal, J.E., & Smith, R.H. (2007). Testing a process-based fine fuel moisture model in two forest types. *Canadian Journal of Forest Research-Revue Canadienne De Recherche Forestiere*, *37*, 23–35.

McArthur, A.G. (1967). Fire behaviour in Eucalypt forests. *Canberra, Leaflet 107*. Department of National Development Forestry and Timber Bureau.

Monteith, J.L., & Unsworth, M.H. (1990). *Principles of environmental physics*. London: Edward Arnold.

Nelson, R. (1984). A method for describing equilibrium moisture content. *Canadian Journal of Forest Research/Revue Canadienne de Recherche Forestiere*, *14*, 597–600.

Nemani, R.R., & Running, S.W. (1989). Estimation of regional surface resistance to evapotranspiration from NDVI and thermal-IR AVHRR data. *Journal of Applied Meteorology*, *28*, 276–284.

Nieto, H., Aguado, I., Chuvieco, E., & Sandholt, I. (2010). Dead fuel moisture estimation with MSG-SEVIRI data. Retrieval of meteorological data for the calculation of the equilibrium moisture content. *Agricultural and Forest Meteorology*, *150*, 861–870.

Nieto, H., Sandholt, I., Aguado, I., Chuvieco, E., & Stisen, S. (2011). Air temperature estimation with MSG-SEVIRI data: Calibration and validation of the TVX algorithm for the Iberian Peninsula. *Remote Sensing of Environment*, *115*, 107–116.

Oyoshi, K., Akatsuka, S., Takeuchi, W., & Sobue, S. (2014). Hourly LST monitoring with the Japanese geostationary satellite MTSAT-1R over the Asia-Pacific region. *Asian Journal of Geoinformatics*, *14*(3), 1–13.

Peterson, S.H., Roberts, D.A., & Dennison, P.E. (2008). Mapping live fuel moisture with MODIS data: A multiple regression approach. *Remote Sensing of Environment*, *112*, 4272–4284.

Prihodko, L., & Goward, S.N. (1997). Estimation of air temperature from remotely sensed surface observations. *Remote Sensing of Environment*, *60*, 335–346.

Prince, S.D., Goetz, S.J., Dubayah, R.O., Czajkowski, K.P., & Thawley, M. (1998). Inference of surface and air temperature, atmospheric precipitable water and vapor pressure deficit using Advanced Very High-Resolution Radiometer satellite observations: Comparison with field observations. *Journal of Hydrology*, *212*, 230–249.

R Development Core Team (2014). R: A language and environment for statistical computing. R Foundation for Statistical Computing, Vienna, Austria. http://www.R-project.org/.

Resco de Dios, V., Fellows, A.W., Nolan, R.H., Boer, M.M., Bradstock, R.A., Domingo, F., & Goulden, M.L. (2015). A semi-mechanistic model for predicting the moisture content of fine litter. *Agricultural and Forest Meteorology*, *203*, 64–73.

Rothermel, R.C. (1983). How to predict the spread and intensity of forest and range fires. *Intermountain Forest and Range Experiment Station, General Technical Report INT-GTR-143* (Ogden, UT).

Smith, W.L. (1966). Note on the relationship between total precipitable water and surface dew point. *Journal of Applied Meteorology*, *5*, 726–727.

Stisen, S., Sandholt, I., Norgaard, A., Fensholt, R., & Eklundh, L. (2007). Estimation of diurnal air temperature using MSG SEVIRI data in West Africa. *Remote Sensing of Environment*, *110*, 262–274.

Stow, D., & Niphadkar, M. (2007). Stability, normalization and accuracy of MODIS-derived estimates of live fuel moisture for southern California chaparral. *International Journal of Remote Sensing*, *28*, 5175–5182.

Sullivan, A.L. (2009). Wildland surface fire spread modelling, 1990–2007. 2: Empirical and quasi-empirical models. *International Journal of Wildland Fire*, *18*, 369–386.

Tucker, C.J. (1979). Red and photographic infrared linear combinations for monitoring vegetation. *Remote Sensing of Environment*, *8*, 127–150.

van Gorsel, E. (2013). Tumbarumba OzFlux tower site OzFlux: Australian and New Zealand Flux Research and Monitoring hdl: 102.100.100/14241.

Vermote, E.F. (2013). *MODIS surface reflectance user's guide*. MODIS Land Surface Reflectance Science Computing Facility.

Viney, N.R. (1991). A review of fine fuel moisture modelling. *International Journal of Wildland Fire*, *1*, 215–234.

Viney, N.R., & Catchpole, E.A. (1991). Estimating fuel moisture response times from field observations. *International Journal of Wildland Fire*, *1*, 211–214.

Viswanadham, Y. (1981). The relationship between total precipitable water and surface dew point. *Journal of Applied Meteorology*, *20*, 3–7.

Wan, Z.M., & Dozier, J. (1996). A generalized split-window algorithm for retrieving land-surface temperature from space. *IEEE Transactions on Geoscience and Remote Sensing*, *34*, 892–905.

Wan, Z.M., Zhang, Y.L., Zhang, Q.C., & Li, Z.L. (2002). Validation of the land-surface temperature products retrieved from Terra Moderate Resolution Imaging Spectroradiometer data. *Remote Sensing of Environment*, *83*, 163–180.

Wu, T.T., & Li, Y.R. (2013). Spatial interpolation of temperature in the United States using residual kriging. *Applied Geography*, *44*, 112–120.

Yebra, M., & Chuvieco, E. (2009). Linking ecological information and radiative transfer models to estimate fuel moisture content in the Mediterranean region of Spain: Solving the ill-posed inverse problem. *Remote Sensing of Environment*, *113*, 2403–2411.

Yebra, M., Dennison, P.E., Chuvieco, E., Riaño, D., Zylstra, P., Hunt, E.R., ... Jurado, S. (2013). A global review of remote sensing of live fuel moisture content for fire danger assessment: Moving towards operational products. *Remote Sensing of Environment*, *136*, 455–468.